Interactions between Substrate Analogues and Heme Ligands in Nitric Oxide Synthase†

Jianling Wang,*,‡ Dennis J. Stuehr,§ and Denis L. Rousseau||

Research Department, Novartis Pharmaceuticals Corporation, Summit, New Jersey 07901, Department of Immunology, NN-1, The Cleveland Clinic, Cleveland, Ohio 44195, and Department of Physiology and Biophysics, Albert Einstein College of Medicine, Bronx, New York 10461

Received September 13, 1996; Revised Manuscript Received January 13, 1997⊗

ABSTRACT: The substrate binding site in nitric oxide synthase (NOS) can accommodate the physiological substrates, L-arginine and N^{ω}-hydroxy L-arginine as well as many substrate analogues and inhibitors. Resonance Raman spectra of carbon monoxide-bound NOS were measured to determine how these substrates and analogues interact with heme, the prosthetic group which activates oxygen for the catalytic generation of NO and citrulline from arginine in the enzyme. Two distinct conformations of the Fe−C−O moiety were detected in the resonance Raman spectra, although in the optical absorption spectra the two species are indistinguishable. In one, termed the β-form, the Fe−CO stretching frequency and the C−O stretching frequency, located at ∼487 and ∼1949 cm^{-1}, respectively, demonstrate that the Fe−C−O group adopts a linear conformation perpendicular to the heme plane ("open" structure). In the other, termed the α-form, frequencies of ∼502 and ∼1929 cm^{-1}, respectively, indicate that the binding properties of bound CO are significantly affected by its immediate environment thereby leading to a "closed" structure. In the presence of L-arginine or N^{ω}-OH-L-arginine all of the molecules exhibit the closed structure, indicating that the substrates exert a strong polar (and/or steric) effect on the heme-bound ligand. In the absence of any substrate or inhibitor only half of the heme population adopts the open structure whereas the rest of the heme content retains the closed conformation. It is proposed that in this population with the closed structure tetrahydrobiopterin, a cofactor of NO synthase, may reside in close proximity to the heme-bound ligand and interact with it in a similar manner as do substrates. The inverse correlation between the Fe−CO and C−O stretching modes suggests that in NOS the bonding of the cysteine to the heme iron may be weaker, as found in chloroperoxidase, than in cytochrome P-450 enzymes. This work continually proves resonance Raman spectroscopy as a powerful probe for the interactions between substrate/inhibitor and the heme active site of proteins.

Nitric oxide (NO), an unstable, diatomic free radical and potentially toxic molecule, has been the subject of a large number of studies recently (Feldman et al., 1993; Ignarro & Murad, 1995; Feelisch & Stamler, 1996) owing to the discovery of the many diverse functional roles it plays in physiology. First, Furchgott (1988), Moncada et al. (1988) and Ignarro et al. (1988) found that NO (or a labile compound releasing NO) is the endothelium-derived relaxing factor (EDRF), the substance which activates soluble guanylyl cyclase (sGC) and induces vascular smooth muscle relaxation. Second, NO is released from cerebellar cells of rat brain, in response to glutamate binding to the *N*-methyl-D-aspartate (NMDA) receptor, which in turn activates sGC, converting guanosine triphosphate (GTP) to cyclic guanosine monphosphate (cGMP) and ultimately serving as a messenger in central and peripheral nervous systems. Finally, Hibbs (1987), Marletta et al. (1988), and Stuehr and co-workers (Stuehr et al., 1989; Stuehr & Nathan, 1989) found that NO also acts as a cytotoxic agent by playing a role in the immune system's ability to kill tumor cells and intracellular parasites. Further studies indicate that this inorganic gas is synthesized, *in vivo*, by a family of enzymes termed nitric oxide synthases (NOSs) found in animals as diverse as barnacles, fruit flies, horseshoe crabs, chickens, trout, and humans (Feldman et al., 1993). It is noteworthy that NO is much more than just another biological messenger in that its trafficking is independent of the specific transporter or channels used by other chemical counterparts. Instead, NO diffuses freely in all directions from its site of origin. The control of synthesis of NO catalyzed by NOSs *in vivo* thus becomes a key issue in regulating its activity and all its physiological functions. The understanding of the nature of NOSs is extremely valuable for both fundamental physiological and practical medicine.

The synthesis of NO catalyzed by NOSs consists of a two-step oxidation of arginine, each of which involves a monooxygenation reaction as found in the catalysis reactions of the cytochrome P-450 class of enzymes (Bredt et al., 1991; Culotta & Koshland, 1992; Lancaster, 1992; Stamler et al., 1992; Snyder & Bredt, 1992; Feldman et al., 1993; Griffith & Stuehr, 1995).

$$\text{L-arginine} \xrightarrow{\text{NOS}} N^{\omega}\text{-OH-L-arginine} \xrightarrow{\text{NOS}} \text{L-citrulline} + \text{NO} \quad (1)$$

Several studies have established the presence of three different isoforms of the enzyme (Förstermann et al., 1993;

† This work is supported by National Institutes of Health grants to D.L.R. (GM48714) and D.J.S. (CA53914, GM51491). D.J.S. is an established investigator of the American Heart Association.

* To whom correspondence should be addressed. Phone: (908) 277−4649. FAX: (908) 277-2405. E-mail: jianling.wang@ussu.mhs.ciba.com.

‡ Novartis Pharmaceuticals Corp.

§ The Cleveland Clinic.

|| Albert Einstein College of Medicine.

⊗ Abstract published in *Advance ACS Abstracts,* March 15, 1997.

S0006-2960(96)02309-4 CCC: $14.00

Sessa, 1994). The neuronal enzyme from rat brain (*b*-NOS), which we use in the present work, and the protein from endothelial cells (*e*-NOS) are constitutive, while the NO synthase purified from macrophage is inducible and cytokine dependent. All the isoforms of NOSs contain FAD and FMN in the reductase domain and tetrahydrobiopterin (BH_4), heme and the binding site for substrate, L-arginine, in the oxygenase domain. The enzymes exist as homodimers in which, as found in recent studies of the macrophage enzyme (Ghosh & Stuehr, 1995), the two subunits align in a head-to-head manner with the oxygenase domains of the two subunits interacting with each other. For the constitutive NOSs the binding of calcium−calmodulin (Ca^{2+}-CaM) near the interface of the two domains facilitates the electron transfer from NADPH to the heme catalytic site during the enzymatic synthesis of NO (Abu-Soud & Stuehr, 1993).

The heme of NOSs is necessary for both steps of monooxygenation reactions involved in the synthesis of NO (see eq 1) (Stuehr & Ikeda-Saito, 1992; Pufahl & Marletta, 1993) and is coordinated by a thiolate proximal ligand (Wang et al., 1993, 1995a; Chen et al., 1994; Richards & Marletta, 1994; McMillian & Masters, 1995). The resting form of NOSs has a high-spin ferric heme iron and the reduced form of NOSs shows a pentacoordinate high-spin (5C/HS) heme, available for the coordination of exogenous ligands such as CO, NO, and CN as well as O_2, the physiological ligand (Wang et al., 1993, 1994, 1995a). Several laboratories have found that BH_4 plays a crucial role in maintaining a stable pocket for the heme catalytic active site (Wang et al., 1995a; Klatt et al., 1996) as well as in stabilizing the dimeric structure of NOSs (Baek et al., 1993; Mayer & Werner, 1995; Tzeng et al., 1995), despite the negative effects recently reported in dimerization of *e*-NOS (Rodriguez-Crespo et al., 1996). In its absence, the enzymes becomes less stable (Hevel & Marletta, 1992) and the heme environment of NOS is substantially perturbed by the coordination of a low-spin ligand to the heme, leading to an inactive form of the enzyme (Wang et al., 1995a). In addition, NOSs are also similar to cytochromes P-450 (Dowson & Sono, 1987; Champion, 1988) by displaying a susceptibility of the spectral properties of heme−exogenous ligand complexes to the presence of substrate (Wang et al., 1994).

The full understanding of the catalytic mechanism of the enzyme requires knowledge of the substrate binding site(s) and the interactions between the substrates and the heme/heme-bound ligands. The CO derivatives of hemeproteins are a unique model for such studies owing to the similar molecular (diatomic) and electronic structure of CO to the physiological ligand, O_2, and the greater stability of the CO−heme iron complexes. Resonance Raman spectroscopy and Fourier transform infrared spectroscopy (FT-IR) offer excellent probes for these due to the rich information they can provide, such as the identity of the proximal ligand, the configuration, and the oxidation state of the heme iron and the interaction of heme with its environment. In addition, the spectra of the CO−heme complexes are very sensitive to the presence of substrates/co-factors and to other changes in the CO binding properties induced by the environment. This is most evident by the observation that the optical spectra of the CO adducts of cytochrome P-450_{cam} are unperturbed by the presence of substrates whereas the CO-associated marker lines in the resonance Raman spectra (Uno et al., 1985; Bangcharoenpaurpong, 1987; Hu & Kincaid, 1991; Wells et al., 1992) and IR spectra (O'Keeffe et al., 1978a; Jung et al., 1992) exhibit substantial changes due to the presence and the identity of the substrates. In particular, the homogeneous and bent/tilted Fe−C−O linkage inferred from Raman and IR data has been confirmed by the X-ray crystallographic data from the CO adduct of camphor-bound cytochrome P-450_{cam} where heme-bound CO has to bend or tilt from the heme normal by 14° in order to accommodate the polar (and/or steric) effect from the substrate, camphor (Raag & Polous, 1989).

The initial characterization on the CO derivative of *b*-NOS by resonance Raman spectroscopy (Wang et al., 1993) showed an Fe−CO stretching mode (ν_{Fe-CO}) with a very low frequency ($\sim$490 cm^{-1}) in comparison to hemeproteins in which histidine is the proximal ligand (Yu & Kerr, 1988; Ray et al., 1994; Wang et al., 1996a), consistent with the coordination by a proximal cysteine (thiolate) residue. In the absence of BH_4 the heme active site of NOSs is significantly destabilized and the bonding between the heme iron and the proximal cysteine is loosened. CO coordination to the heme causes a gradual dissociation of the *trans* cysteine residue thereby leading to a switch of the proximal ligand (to a histidine residue) (Wang et al., 1995a). In addition, in the absence of exogenous substrates such as L-arginine or N^{ω}-OH-L-arginine (substrate-free form), ν_{Fe-CO} is found to be quite broad, indicating the presence of multiple ligand binding active sites for NOSs. Although the effects of substrates on the heme iron−CO binding properties is still unclear, we found that the presence of L-arginine (L-Arg) appreciably stabilizes the coordination of NO to the ferrous heme iron and also alters the binding properties of the Fe−N−O linkage (Wang et al., 1994). All of these suggest strong interactions between substrates/cofactors and heme/heme-bound ligands and also implicate a close proximity of bound substrate to the heme active site of NOSs.

In this work we extend our previous investigation on the substrate-dependent structural perturbations of the heme-ligand active site by studying the effects of substrates (e.g., L-Arg, N^{ω}-OH-L-Arg) and L-arginine-like inhibitors (L-citrulline and L-thiocitrulline) (Figure 1) on the binding properties and dynamics of CO derivatives of *b*-NOS(+2). We have also compared the resonance Raman scattering results from NOS−CO complexes with those from the CO adducts of cytochromes P-450 which show structural sensitivity to the presence and identity of substrates and whose crystal structures are known. Our data demonstrate that in the absence of substrates, bound CO exhibits a wide distribution of conformations suggesting an open distal pocket. In the presence of substrate, a strong polar (or steric) effect is exerted on the bound CO.

MATERIALS AND METHODS

The constitutive NOS from rat brain was purified by sequential chromatography on 2′,5′-ADP Sepharose and Mono Q anion exchange resin as described previously (Stuehr & Ikeda-Saito, 1992). Chloroperoxidase (CPO) was purchased from Sigma and used without further purification. The isotopically labeled CO gases ($^{13}C^{16}O$, $^{12}C^{18}O$, and $^{13}C^{18}O$) were products of ICON (>99%,99% labeled). The reduced form of NOS or CPO was prepared by anaerobically adding dithionite solution to the previously degassed enzyme, from which the CO adducts were generated by exposure of

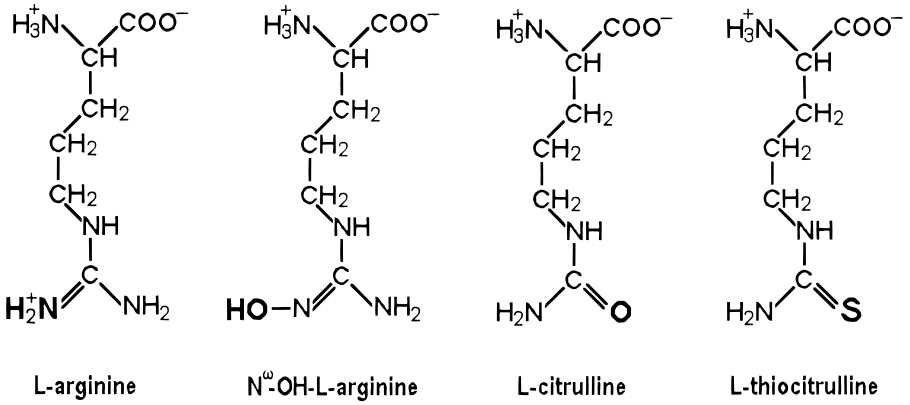

FIGURE 1: Molecular structure of several substrates and inhibitors of nitric oxide synthase.

the samples to either natural $^{12}C^{16}O$ (Matheson, >99% purity) or a stable isotope $^{13}C^{16}O$, $^{12}C^{18}O$, or $^{13}C^{18}O$ (Wang et al., 1993). All of the samples were buffered by 40 mM Hepes, pH 7.4, containing 2 μM BH_4 and 3 mM dithiothreitol (DTT).

The resonance Raman instrumentation used in present study has been described elsewhere (Wang et al., 1996a). Typically, the sample aliquots (100 μL, 20−40 μM) sealed in a rotating cell were irradiated at extremely low laser power (~0.3 mW) to minimize the photoinduced dissociation of heme-bound CO. The excitation wavelength of the helium−cadmium laser used in the present study (441.6 nm) is very close to the Soret maxima of CO adducts of NOS or CPO (~446 nm) and thus greatly enhanced the intensities of the resonance Raman spectra of them. The scattered light was dispersed by a 1.25-m monochromator and detected by a CCD camera. Some of the spectra are base line corrected, but none was smoothed. Optical absorption data were recorded, on a SLM Aminco DW2000 UV−vis spectrophotometer, both prior to and after each Raman measurement to ensure the formation and stability of the CO adducts during the measurements. The frequencies of the Raman shifted lines were calibrated against the lines from indene (Aldrich) (150−1800 cm^{-1}) as well as those from acetone (1709.7 cm^{-1}) and potassium ferrocyanide (2056.7 and 2091.7 cm^{-1}).

RESULTS

Figure 2 depicts the resonance Raman spectra of CO adducts of dithionite-reduced *b*-NOS in its substrate-free form (trace a), L-Arg-bound form (trace b), and N^{ω}-OH-L-Arg-bound form (trace c). The substrate-free form exhibits a spectrum that is similar to that which we reported previously (Wang et al., 1993). Specifically, this species displays a weak line for the Fe−C−O bending mode (δ_{Fe-C-O}) at 562 cm^{-1} and a strong and broad line for ν_{Fe-CO} at ~491 cm^{-1}, which was deconvoluted into two components centered at 487 and 501 cm^{-1}. The addition of substrates such as L-Arg or N^{ω}-OH-L-Arg to *b*-NOS dramatically alters the resonance Raman spectra. The broad line from ν_{Fe-CO} at 491 cm^{-1} in the substrate-free species is replaced by a sharp line at 503 cm^{-1} (for L-Arg) or 502 cm^{-1} (for N^{ω}-OH-L-Arg) and the δ_{Fe-C-O} line (at 562−565 cm^{-1}) is greatly intensified. The slight shift in frequency (~2 cm^{-1}) of the δ_{Fe-C-O} line upon the binding of substrate and its intensification were also reported in the CO complexes of cytochrome P-450_{cam} (Uno et al., 1985). In addition to the changes in the CO-associated marker lines (e.g., ν_{Fe-CO} and δ_{Fe-C-O}), the presence of substrates significantly strengthens the Raman signals from porphyrin macrocycle vibrations (e.g., 393, 407, 691, and 801 cm^{-1}) as well, as evident in the difference spectrum

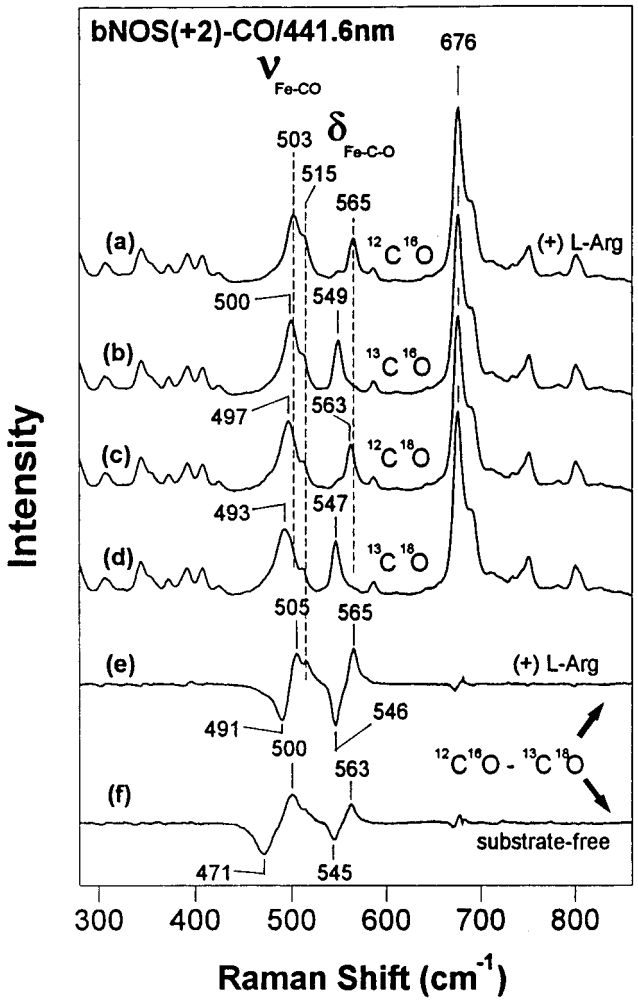

FIGURE 2: Effects of substrates or inhibitors on the low-frequency resonance Raman spectra of the CO adducts of dithionite-reduced *b*-NOS. Spectrum a was obtained from the substrate-free form of the enzyme and traces b−e were from samples containing 2−4 mM L-arginine (b), N^{ω}-OH-L-Arg (c), L-citrulline (d), and L-thiocitrulline (e). The binding of L-Arg or N^{ω}-OH-L-Arg in the distal pocket greatly perturbed the Fe−C−O spectra, but in the presence of L-citrulline or L-thiocitrulline a spectrum that is similar to that from its substrate-free form was obtained. Trace f is the difference between the spectrum from the L-Arg-bound form (b) and that from the substrate-free form (a). In order to minimize photo-induced dissociation of CO, all the spectra were recorded at extremely low laser power (0.3−0.5 mW) (441.6 nm). The buffer solution contains 2 μM BH_4 and 3 mM DTT.

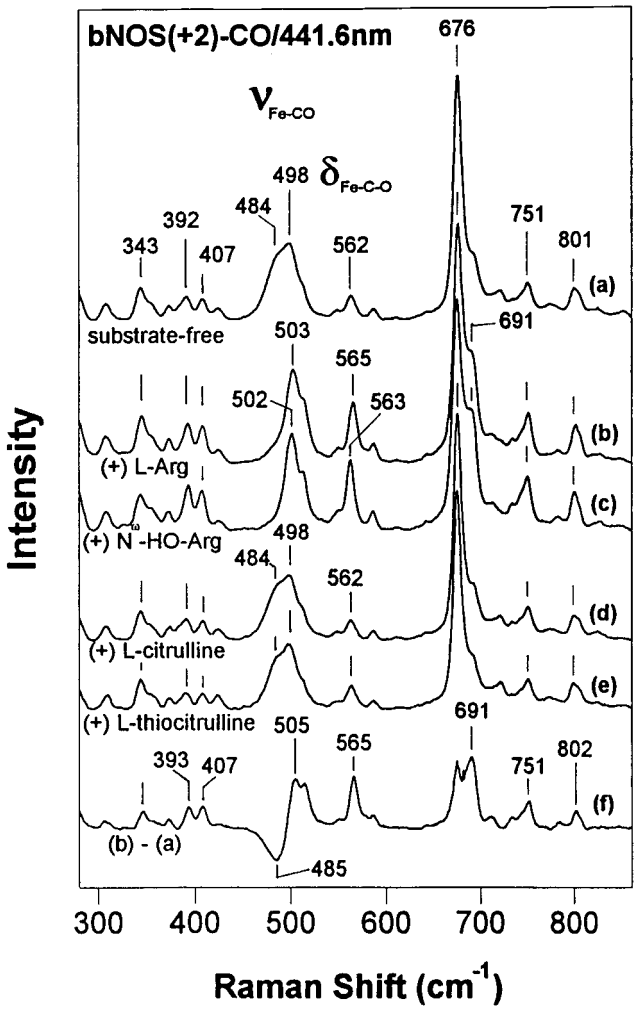

FIGURE 3: Isotopic shifts of resonance Raman lines (in the low-frequency region) of the CO adducts from reduced *b*-NOS in the presence of 2 mM L-Arg. Spectra a−d were from $^{12}C^{16}O$- (a), $^{13}C^{16}O$- (b), $^{12}C^{18}O$- (c), and $^{13}C^{18}O$-bound (d) forms of *b*-NOS. Trace e is the difference spectrum of spectra a minus d ($^{12}C^{16}O - {}^{13}C^{18}O$) where the contributions from porphyrin modes balance out, revealing the isotopic shifts from the Fe−CO stretching (∼503 cm^{-1}) and Fe−C−O bending (565 cm^{-1}) modes. Trace f is a similar difference spectrum of $^{12}C^{16}O$ minus $^{13}C^{18}O$ adducts but was obtained from the substrate-free form of *b*-NOS. The experimental conditions are the same as those described in Figure 2.

(trace f). They may arise from changes in the doming of the porphyrin or in its peripheral groups as a direct consequence of the binding of substrates, although the confirmation of these conclusions requires additional evidence.

In contrast to the effect of L-arginine and N^{ω}-OH-L-arginine, the spectra of *b*-NOS(+2)−CO in the presence of L-citrulline (trace d) and L-thiocitrulline (trace e) are the same as that of the substrate-free species. The binding of L-thiocitrulline, a potent inhibitor for NOSs, (or L-citrulline) to fully oxidized *b*-NOS appreciably alters its resonance Raman (Wang et al., unpublished results) and optical absorption (Frey et al., 1994) and EPR (Salerno et al., 1995) spectra, indicating a strong interaction with the ferric heme iron of NOS. Such interactions result in the inhibition of the enzyme via either blocking the ligand binding site or affecting the redox potential of the heme iron (Abu-Soud et al., 1994; Wang et al., unpublished results). The similarities of the Raman spectra of the CO adducts of the substrate-free form and the L-thiocitrulline-bound (or L-citrulline-bound) form (see Figure 2) implicate a similar immediate environment experienced by the bound CO in both forms. However, we cannot determine from the current data if the CO and the L-thiocitrulline (or L-citrulline) cannot both bind simultaneously or if the L-thiocitrulline does bind but does not perturb the heme−CO structure.

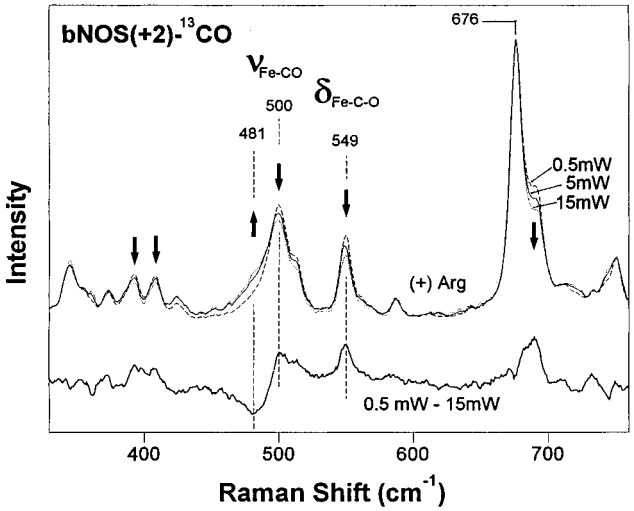

FIGURE 4: Laser power dependence of the low-frequency resonance Raman spectra of the ^{13}CO adduct from reduced *b*-NOS in the presence of 2 mM L-Arg. The spectra were obtained at 0.5 (- - -), 5 (—), or 15 mW (•••) of incident laser power. The arrows designate the direction of increase in laser power. The bottom spectrum is the difference of the spectrum recorded at low power (0.5 mW) minus that recorded at high power (15 mW). The experimental conditions are the same as those described in Figure 2.

The assignments of lines near 500 and 565 cm^{-1} in the spectrum of L-Arg-bound *b*-NOS(+2)−CO have been established by utilizing multiple isotopically labeled CO as shown in Figure 3. Substitution of ^{12}CO by ^{13}CO (trace b) shifts both lines: from 503 to 500 cm^{-1} and from 565 to 549 cm^{-1}. The replacement of the oxygen atom in CO by ^{18}O (trace c), however, decreases only the frequency of the 503 cm^{-1} line (to 497 cm^{-1}). In the presence of doubly labeled CO ($^{13}C^{18}O$) (trace d), both lines are significantly down-shifted by 10 cm^{-1} (to 493 cm^{-1}) and 18 cm^{-1} (to 547 cm^{-1}). The isotope-induced frequency changes of the two lines are more apparent in the difference spectra between spectra from the $^{12}C^{16}O$-bound forms and those from the $^{13}C^{18}O$-bound counterparts (traces e and f). It should be noted that for the same isotopic substitution ($^{12}C^{16}O$ to $^{13}C^{18}O$) the substrate-free form of the enzyme shows a much greater apparent shift in the difference spectrum for the line near 500 cm^{-1} (trace f, ∼29 cm^{-1}) than the L-Arg bound species (trace e, 14 cm^{-1}). As discussed previously (Wang et al., 1993) the large shift in the difference spectrum is a consequence of the presence of two lines separated by about 15 cm^{-1} and both shifting by an amount comparable to the separation. Thus, in the difference spectrum only the lowest and the highest frequency components appear with the other components canceling out.

The resonance Raman spectra from CO-bound *b*-NOS-(+2) is sensitive to the power of the excitation laser (see Figure 4). As a consequence of photodissociation of CO from heme iron, an increase in the laser power (from 0.5 to 15 mW) leads to the weakening of both the δ_{Fe-C-O} line at 549 cm^{-1} and the higher frequency component of ν_{Fe-CO} at

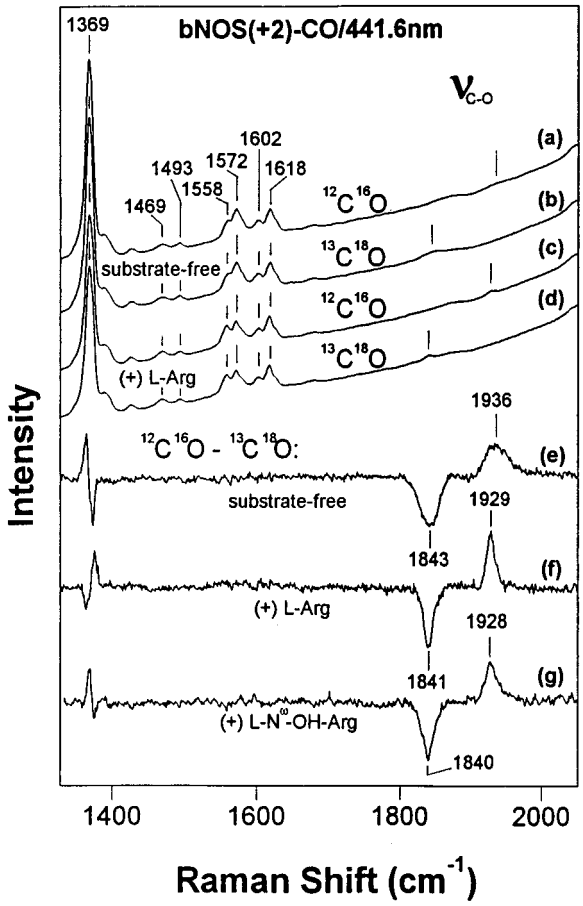

FIGURE 5: Resonance Raman spectra of the CO adducts of reduced *b*-NOS in the high-frequency and ν_{C-O} regions. Spectra a and b are of the $^{12}C^{16}O$ and $^{13}C^{18}O$ adducts of substrate-free *b*-NOS, while traces c and d are of $^{12}C^{16}O-$ and $^{13}C^{18}O-$NOS(+2) in the presence of 2 mM L-Arg. Traces e−g are the differences of spectra of the $^{12}C^{16}O$-bound forms minus those of the $^{13}C^{18}O$-bound species from substrate-free (e), L-Arg-bound (f), and N^{ω}-OH-L-Arg-bound (g) forms of the enzyme. The C−O stretching mode is evident in 1800−2000-cm^{-1} region. The experimental conditions are the same as those described in Figure 2.

500 cm^{-1} in the spectrum of L-Arg-bound *b*-NOS-$^{13}C^{16}O$. However, the laser power increase results in an intensification of the lower frequency species of ν_{Fe-CO} at 481 cm^{-1}. In addition, the photolysis of heme-bound CO in the sample is associated with the variations in the porphyrin macrocycle as evident by the changes in intensity of porphyrin lines (e.g., 393, 407, and 691 cm^{-1}) (also see the difference spectrum at the bottom in Figure 4). A similar difference spectrum has been obtained from the power dependent experiments of *b*-NOS(+2)−CO in the absence of substrate (data not shown). The laser induces a conversion in the Fe−C−O binding geometry from a conformation possessing a higher Fe−CO bond order ($\nu_{Fe-CO} = \sim 500$ cm^{-1}) to a species with weaker Fe−CO bond strength ($\nu_{Fe-CO} = \sim 481$ cm^{-1}).

The binding properties of the CO to the reduced heme of *b*-NOS have been examined in the high-frequency region containing the C−O stretching (ν_{C-O}) mode (Figure 5). The appearance of ν_4, an oxidation state marker line, at 1369 cm^{-1} [for the six-coordinate low-spin (6C/LS) CO-bound reduced heme] and the absence of any contribution at 1347 cm^{-1} (5C/HS) indicate that the spectra are dominated by the CO-bound form of *b*-NOS(+2) (traces a−d) (Wang et al., 1993). The contributions of other porphyrin macrocycle modes such as ν_3 and ν_2 from the CO adducts are apparent

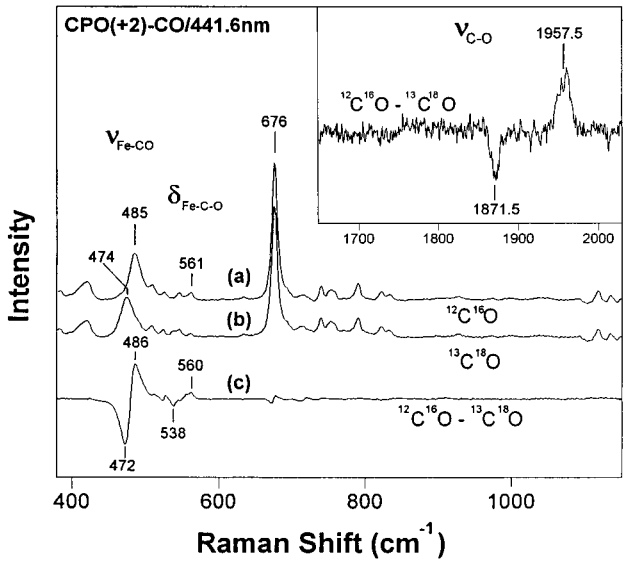

FIGURE 6: Resonance Raman spectra of the CO adducts from reduced chloroperoxidase in the low-frequency and ν_{C-O} (inset) regions. Spectra a and b were from $^{12}C^{16}O$ and $^{13}C^{18}O$ adducts of dithionite-reduced CPO, respectively. Trace c is the difference spectrum of $^{12}C^{16}O$-bound minus $^{13}C^{18}O$-bound CPO(+2) in the $\nu_{Fe-CO}/\delta_{Fe-C-O}$ region. The inset is the same difference but in the ν_{C-O} region. The samples were dissolved in 100 mM phosphate buffer, pH 6.1, and excited at 441.6 nm (4 mW).

at 1493 and 1572 cm^{-1}, respectively, as previously reported (Wang et al., 1993, 1995a). Similar to those observed in the low-frequency region, the presence of L-Arg also intensifies the porphyrin mode at 1558 cm^{-1}. However, this change does not occur in the sample containing N^{ω}-OH-L-Arg (data not shown). This line exhibits no isotopic substitution sensitivity and thus probably originates from the porphyrin mode, ν_{11}, consistent with such an assignment in other heme proteins (Dasgupta et al., 1989; Spiro et al., 1990; Wang et al., 1992). It should be noted that the difference spectrum (trace e) between the natural and isotopically labeled CO adducts of *b*-NOS(+2) in the absence of substrate displays a clear shift of ν_{C-O}. The frequency of ν_{C-O} in the $^{12}C^{16}O$ adduct is at 1936 cm^{-1} and is very broad (half-width $\Gamma_{1/2} = \sim 35$ cm^{-1}). The presence of L-arginine (trace f) and N^{ω}-OH-L-Arg (trace g) causes the frequency of the center of the ν_{C-O} band to shift down by 7 cm^{-1} (for L-Arg) and 8 cm^{-1} (for N^{ω}-OH-L-Arg) and the line to become substantially narrower ($\Gamma_{1/2} = \sim 14$ and ~ 18 cm^{-1}, respectively).

As a model for the catalytic active site of nitric oxide synthase, the binding properties of CO in CPO(+2)−CO, which also possesses a cysteine proximal ligand (Champion, 1988; Wang et al., 1993, 1995a, 1996a), was carried out in the ν_{Fe-CO} and ν_{C-O} regions (Figure 6). The low-frequency spectra from $^{12}C^{16}O$ (trace a) and $^{13}C^{18}O$ adducts of reduced chloroperoxidase (trace b) are consistent with a previous study (Hu & Kincaid, 1993), showing a strong and sharp ν_{Fe-CO} at 485 cm^{-1} and a weak line at 560 cm^{-1} for the Fe−C−O bending mode (trace c). Here we also report the ν_{C-O} frequency at 1957.5 cm^{-1} from the difference spectrum between the $^{12}C^{16}O$ and $^{13}C^{18}O$ adducts of CPO (inset of Figure 6). We found that the frequency of ν_{C-O} from CPO−CO is much higher than those from *b*-NOS−CO samples and that the bandwidth (16 cm^{-1}) of ν_{C-O} from CPO−CO is quite small (Table 1) in comparison to that from the substrate-free form of *b*-NOS−CO but similar to those of *b*-NOS−CO in the presence of substrates (Figure 5).

Table 1: Frequencies of Raman Lines from CO Adducts of *b*-NOS, P-450s, and CPO[a] (in cm^{-1})

protein	no. in figure 8	substrates/inhibitors	form	ν_{Fe-CO} (isotope shift)	$\Gamma_{1/2[Fe-CO]}$	δ_{Fe-C-O} (isotope shift)	ν_{C-O} (isotope shift)	$\Gamma_{1/2[C-O]}$	ref
b-NOS	1A	none	β	487 (∼10)	27	[562 (18)]	1949 (93)	27	*b, c*
	1B		α	501 (∼10)	15	562 (18)	1930 (93)	23	*b, c*
	2	L-arginine	α	503 (10)	17	565 (19)	1929 (88)	14	*c*
	3	N^{ω}-OH-L-Arg	α	502 (11)	15	563 (18)	1928 (88)	18	*c*
	4	L-citrulline	α/β	484/498[1]		562			*c*
	5	L-thiocitrulline	α/β	484/498[1]		562			*c*
P-450	6A	none	β	464	∼31(main)	(556)	1963	∼31 (50)	*d−g*
	6B		α	∼480	(sh)	556	1940	(50)	*d−g*
	7	norcamphor	α	473			1947	10	*g−h*
	8	adamantanone	α	474			1955	9	*g−h*
	9	CPRQ	α	476			1941	∼11	*g, i*
	10	fenchone	α	480			1945	11	*g, i*
	11	camphor	α	481		558	1940	13	*d−h*
	12	TMCH	α	485	9.7		1934	10	*g, i*
CPO	13	pH ∼3.3		488−492	∼25	ND	1942		*f, j−k*
	14	pH ∼6.1		485 (11)	16	560 (22)	1957.5 (86)	16	*c, f, k*

[a] δ_{Fe-C-O}, ν_{Fe-CO}, and ν_{C-O} are the Fe−C−O bending, Fe−CO stretching, and C−O stretching modes, respectively. $\Gamma_{1/2}$ represents the full-width at half height. The isotope shifts are the frequency differences between the $^{12}C^{16}O$ and the $^{13}C^{18}O$ derivatives. For ν_{Fe-CO}, they were measured from the absolute spectra of the $^{12}C^{16}O$- and $^{13}C^{18}O$-bound forms of NOS(+2) obtained at the excitation wavelength of 441.6 nm. [b] Wang et al., 1993. [c] This work. [d] Wells et al., 1992. [e] Uno et al., 1985. [f] O'Keeffe et al., 1978a. [g] Jung et al., 1992. [h] Hu & Kincaid, 1991. [i] Bangcharoenpaurpong, 1987. [j] Bangcharoenpaurpong et al., 1986. [k] Hu & Kincaid, 1993. [l] For samples containing L-citrulline or L-thiocitrulline, the Raman spectra of NOS(+2)−CO are virtually the same as that from the substrate-free species.

DISCUSSION

Assignment of Three CO-Associated Marker Lines. Three CO-associated marker lines are detected for the CO adducts of *b*-NOS in both the substrate-free and substrate-bound forms. The two lines at ∼500 and ∼565 cm^{-1} have been reported previously for the substrate free form and tentatively assigned as the Fe−CO stretching (ν_{Fe-CO}) and Fe−C−O bending modes (δ_{Fe-C-O}), respectively (Wang et al., 1993). In the present work, the assignments of these lines are unequivocally established by the utilization of multiple isotopically substituted CO. Specifically, the line near 500 cm^{-1} (e.g., 503 cm^{-1} for L-Arg-bound form in Figure 3) exhibits a monotonous decline in the frequency with respect to the increase in the mass of bound CO (from $^{12}C^{16}O$ to $^{13}C^{16}O$, $^{12}C^{18}O$, and $^{13}C^{18}O$), thereby confirming the assignment of this line as ν_{Fe-CO} (Table 1). In contrast, the line near 565 cm^{-1} only displays a zigzag pattern in frequency, establishing its assignment as the Fe−C−O bending mode,[1] as found in other heme proteins (Benko & Yu, 1983). It should be noted that our results clearly preclude the shoulder (∼515 cm^{-1}) of ν_{Fe-CO} as originating from another component of ν_{Fe-CO} due to the insensitivity of its frequency to CO isotopic substitution (traces a−d in Figure 3). We attribute the appearance of a shoulder on the 505-cm^{-1} line (at 515 cm^{-1}) in the $^{12}C^{16}O-^{13}C^{18}O$ difference spectrum (trace e) as originating from the enhancement of Fermi resonance coupling due to the similar frequencies for both (Proniewicz & Kincaid, 1990; Wang et al., 1995c). As ν_{Fe-CO} shifts away from it by applying labeled CO, this effect is expected to diminish. That this shoulder becomes much weaker in the $^{13}C^{16}O-^{13}C^{18}O$ and $^{12}C^{18}O-^{13}C^{18}O$ difference spectra (data not shown) and that the shoulder is completely absent in the negative trough at 491 cm^{-1} (in $^{12}C^{16}O - ^{13}C^{18}O$ difference spectrum, trace e) strongly support this argument.

The C−O stretching mode of heme proteins appears in the high-frequency region (1800−2200 cm^{-1}) (Yu & Kerr, 1988; Sampath et al., 1996; Wang et al., 1996a). In the three CO adducts of ferrous *b*-NOS that we examined (substrate-free form, L-Arg-bound form, and N^{ω}-OH-L-Arg-bound form), a line near 1930 cm^{-1} has been detected for $^{12}C^{16}O$ (traces e−g in Figure 5) which shifts to ∼1840 cm^{-1} upon the substitution by $^{13}C^{18}O$. We assign the line as ν_{C-O} since both its frequency (∼1930 cm^{-1}) and the magnitude in the isotopic shift (∼90 cm^{-1}) of the line are similar to those reported in cytochrome P-450_{cam}, CPO (Table 1; O'Keeffe et al., 1978a; Jung et al., 1992), and other heme proteins (Yu & Kerr, 1988; Ray et al., 1994; Wang et al., 1995b,c, 1996a).

Multiple CO-Binding Conformations. The substrate-free form of *b*-NOS(+2)−CO has very broad ν_{Fe-CO} (∼491 cm^{-1}) and ν_{C-O} lines (∼1936 cm^{-1}) in comparison to those from its substrate-bound counterparts (Figures 2 and 5 and Table 1) and other heme proteins (Yu & Kerr, 1988; Jung et al., 1992; Ray et al., 1994; Want et al., 1996a). We have carried out a spectral deconvolution in the two regions, as shown in Figure 7, in which the position, line width, and Gaussian/Lorentzian ratio of the lines were unconstrained. In the low-frequency region the spectral deconvolution results indicate the existence of two componments with CO isotope sensitivity and a porphyrin contribution near 515 cm^{-1} in the substrate-free form of *b*-NOS(+2)−CO (Figure 7A). The two ν_{Fe-CO} species were identified at 486.7 and 501.0 cm^{-1}, similar to those which we reported previously (Wang et al., 1993). In the ν_{C-O} region (Figure 7B) two forms are apparent at 1930.0 and 1949.2 cm^{-1} as well. Interestingly, the two species are interconvertable by either varying the excitation laser power (Figure 4) or by adding L-arginine-like substrates or inhibitors (Figure 2). For example, the addition of L-Arg or N^{ω}-OH-L-Arg to the substrate-free form

[1] Kitagawa and co-workers (Hirota et al., 1994) recently suggested that a newly detected line at ∼360 cm^{-1} might originate from the fundamental of the Fe−C−O bending mode and that the line at 560−570 cm^{-1} is possibly a combination of the ∼360-cm^{-1} line with a porphyrin mode. For CO adducts of *b*-NOS, as evident in the difference spectra (traces e and f in Figure 3), no line in the 250−450-cm^{-1} region shows isotopic sensitivity. Therefore, we accept the original assignment in which the line at 565 cm^{-1} is the fundamental bending mode.

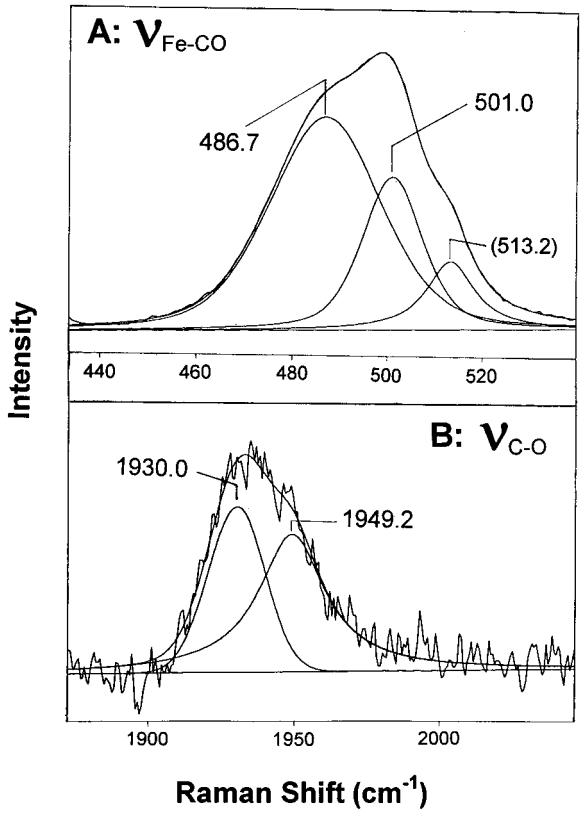

FIGURE 7: Spectral deconvolution of the resonance Raman data from the substrate-free form of *b*-NOS(+2)−CO in the ν_{Fe-CO} (a) and ν_{C-O} regions (b). In the computer curve fitting, neither the position, nor the width, nor the Gaussian/Lorentzian ratio of the lines was constrained. The line at 513.2 cm^{-1} in the top panel does not originate from a CO-associated vibration.

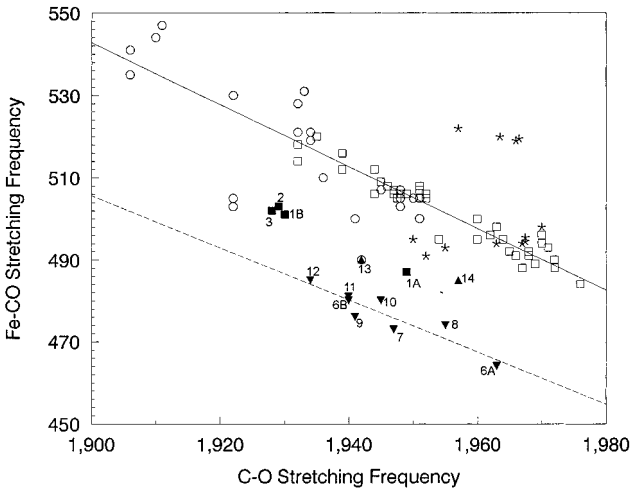

FIGURE 8: Correlation between the ν_{Fe-CO} and ν_{C-O} frequencies. The squares represent proteins containing a proximal histidine (or imidazole) such as hemoglobins, myoglobins, and porphyrins with neutral imidazoles, and the circles correspond to peroxidases. The solid line is the correlation curve for those proteins. The family of terminal oxidases is indicated by the asterisks. Proteins possessing a proximal cysteine ligand are indicated by the darkened symbols and include cytochromes P-450 (wedges), chloroperoxidase (triangles), and nitric oxide synthases (squares). The dashed line is the correlation curve for the P-450s and the data points from *b*-NOS and CPO locate above the P-450s curve. The numbering of the points correspond to the those listed in Table 1.

of *b*-NOS(+2)−CO narrows and shifts both the ν_{Fe-CO} and ν_{C-O} lines (Figures 2 and 5), leading to a single species having ν_{Fe-CO} at ∼502 cm^{-1} and ν_{C-O} at ∼1929 cm^{-1}. In addition, the isotopic shift of ν_{Fe-CO} (14 cm^{-1}) observed from the difference spectrum of $^{12}C^{16}O$-bound minus $^{13}C^{18}O$-bound *b*-NOS in the presence of L-Arg (trace e in Figure 3) is consistent with a single CO-binding conformation. It also supports the proposal that two CO-bound species are present in the substrate-free form of NOS(+2)−CO which we made in a previous study on the basis of an anomalously large shift of ν_{Fe-CO} (∼29 cm^{-1}) obtained in the $^{12}C^{16}O - {}^{13}C^{18}O$ difference spectrum [trace f in Figure 3 and Wang et al. (1993)]. We conclude that the ν_{Fe-CO} at 501.0 cm^{-1} and ν_{C-O} at 1930.0 cm^{-1} originate from the same species, which we term the α-form here. We assign this same structure to the L-Arg and the N^{ω}-OH-L-Arg-bound forms (Table 1) owing to the similar frequencies and line widths of ν_{Fe-CO} and ν_{C-O}. The Fe−C−O binding conformation showing ν_{Fe-CO} at low frequency (486.7 cm^{-1}) and ν_{C-O} at higher frequency (1949.2 cm^{-1}) in the substrate-free form of *b*-NOS−CO is termed as the β-form. The origin of these forms will be described in a subsequent section.

The identification of multicomponent Fe−CO binding conformations were reported for cytochromes P-450 and CPO (Table 1). FT-IR studies on the substrate-free form of P-450$_{cam}$ revealed a broad line for ν_{C-O} which led to at least two distinct species of ν_{C-O} (O'Keeffe et al., 1978a; Jung et al., 1992). The ν_{Fe-CO} signal in the resonance Raman spectrum of the substrate-free form of P-450 is also quite broad (∼31 cm^{-1}) with a main peak at 464 cm^{-1} and a shoulder near ∼480 cm^{-1} (Uno et al., 1985). Here we also classify them into α- or β-forms, in a similar manner as we used for *b*-NOS, and summarize the assignments in Table 1. For chloroperoxidase, conformational switching of the Fe−C−O linkage was also detected by altering the pH (O'Keeffe et al., 1978a; Hu & Kincaid, 1993) despite the absence of the involvement of substrates in that protein.

ν_{Fe-CO}/ν_{C-O} Correlation. The frequency of ν_{Fe-CO} is correlated with that of ν_{C-O} owing to the binding properties of the proximal ligand−Fe−C−O linkage (Yu & Kerr, 1988; Rousseau et al., 1993; Ray et al., 1994; Wang et al., 1995b, 1996a). Carbon monoxide, possessing ten valence electrons, is a σ-donor and a π-acceptor. It binds to heme iron via the donation of electron density from its lone pair to the iron d_{z^2} orbital (σ-bond) and via the back-donation from the iron d_{π} orbitals to the CO empty π* orbital (π-bond) (Yu & Kerr, 1988; Rousseau et al., 1993; Ray et al., 1994; Wang et al., 1995b, 1996a). Such coordination allows the bond order of Fe−CO to be correlated with that of C−O, with respect to the changes in the structural environment. For heme proteins containing the same type of proximal ligand, the distribution of the π-electron density within the Fe−C−O linkage is susceptible to the polar or steric environment around bound CO in the distal pocket (Ray et al., 1994; Li et al., 1994; Kushkuley & Stavrov, 1996). The structural effects promoting π-back-bonding strengthen the Fe−CO bond order (i.e., a frequency increase in ν_{Fe-CO}) and also weaken C−O bond strength due to the increase in the electron density in the CO antibonding orbital. This allows the establishment of a well-known correlation between the frequencies of ν_{Fe-CO} and ν_{C-O} (Figure 8) in which the variations in the immediate environment of the bound CO result in changes in frequencies of ν_{Fe-CO} and ν_{C-O} (Ray et al., 1994; Wang et al., 1995b, 1996a). A highly polar environment favors the π-back-donation and thus moves the ν_{Fe-CO}/ν_{C-O} frequencies along the curve toward the left. In addition, the frequencies of

ν_{Fe-CO} and ν_{C-O} and the correlation between them are able to serve as a probe for the identity or properties of the proximal ligand since CO interacts with the proximal ligand by competing for the same orbital (iron d_{z^2}) to bind the heme iron (σ-bond). As a result of such competition, coordination of an electron-rich proximal residue on the *trans* side will substantially weaken the σ-bonding between the heme iron and bound CO which in turn lowers only the frequency of ν_{Fe-CO} without greatly altering that of ν_{C-O}. As a result, the CO derivatives of hemeproteins or porphyrins possessing a similar proximal ligand (e.g., histidine, imidazole) lie on the same correlation curve (solid line in Figure 8) while those in cytochromes P-450 having a proximal thiolate lie along a different curve (broken line).

In both cytochromes P-450 and CPO, cysteine has been identified as the proximal ligand (Poulos et al., 1985; Champion, 1988). However, as may be seen from Figure 8, CPO is displaced from the P-450 correlation curve. This was attributed to a weaker Fe−S linkage (Bangcharoenpaurpong et al., 1986), possibly due to less electron donation from the thiolate ligand in CPO than in the P-450s. Indeed, a weaker Fe−S bond ($\nu_{Fe-S} = 347$ cm^{-1}) was found, from the ferric high-spin heme, in CPO (Champion et al., 1982) than in P-450$_{cam}$ ($\nu_{Fe-S} = 351$ cm^{-1}) (Bangcharoenpaurpong et al., 1986), which may be related to the distinct orientation of the proximal helices between the two proteins (Poulos, 1996). It is now well established that the iron in *b*-NOS is coordinated on the proximal side by cysteine (Stuehr & Ikeda-Saito, 1992; McMillan et al., 1992; Wang et al., 1993, 1995a, 1996a). When the cysteine residue predicted as the candidate for the proximal ligand in *e*-NOS (Cys-184) (Chen et al., 1994) or *b*-NOS (Cys-415) (Richards & Marletta, 1994; McMillian & Masters, 1995) is removed by site-directed mutagenesis, NO synthases lose the absorption bands from the heme, indicating loss of the heme as a consequence of the disruption of the bonding between heme iron and apoprotein via the cysteine residue. All of the ν_{Fe-CO}/ν_{C-O} data from *b*-NOS on which we are reporting here lie above the cytochrome P-450 correlation curve. Thus, as found in CPO, a weaker interaction between heme iron and the proximal cysteine is anticipated in *b*-NOS than in P-450s evident by the displacement of its correlation data from that for the P-450s. Although a new correlation line above that from P-450s may be drawn that includes the current *b*-NOS and the CPO data, we are reluctant to do so at present as it is derived from a small body of data. When a larger data set is obtained the correlation should be re-evaluated. A measurement of the Fe−S stretching frequency by Raman scattering to obtain an indication of the Fe−S bond strength should also help to clarify this issue.

Origin of Multiple Ligand-Binding Conformers. The origin of the two Fe−CO conformations in the substrate-free form of *b*-NOS is quite intriguing. In a previous report (Wang et al., 1993), we were able to exclude contamination from *b*-NOS$_{420}$, a cytochrome P420-like denatured product of *b*-NOS (Wang et al., 1995a), as the optical absorption spectrum indicated only an insignificant population of the *b*-NOS$_{420}$ species (<10%) and also the resonance Raman spectra obtained by exciting at 441.6 nm selectively enhanced only the active form of the enzyme (Soret at 445 nm) but not the *b*-NOS$_{420}$ form, and therefore neither of the lines can originate from the *b*-NOS$_{420}$ form. In addition, as there are differences in both the CO-associated marker lines and modes from the porphyrin macrocycle, between the spectrum of the native enzyme (active form: *b*-NOS$_{450}$) in the substrate-free form and that of *b*-NOS$_{420}$ (Wang et al., 1995a), lines from the *b*-NOS$_{420}$ form would appear in other regions of the spectrum. Changes in the identity or properties of the proximal ligand could also lead to a significant difference in the Fe−CO bond order as we discussed above. This interpretation, however, is very unlikely since the optical data from the substrate-free form of *b*-NOS(+2)−CO (mixture of α- and β-forms) are identical to those from the substrate bound form (only α-form) but changes in the proximal ligand would be expected to affect the optical spectrum.

Another possibility for the origin of the two forms arises from the similarity of the ν_{Fe-CO} and ν_{C-O} frequencies from the α-form of the substrate-free enzyme with those from α-form of the substrate-bound *b*-NOS (Table 1). It could be argued that this observation suggests the presence of substrate-bound forms in our "substrate-free" samples. However, chromatographic analysis did not show the presence of L-arginine or N^{ω}-OH-L-Arg, thereby precluding an equal mixture of the substrate-free and the substrate-bound forms. Furthermore, EPR spectra of the resting enzyme have ruled out the presence of any bound L-arginine (Salerno et al., 1995). In cytochrome P-450$_{cam}$, the ν_{Fe-CO} and ν_{C-O} frequencies for one of the two equal species (α-form) present in the substrate-free enzyme also coincide with those from the substrate-bound counterpart (O'Keeffe et al., 1978a). It was not attributed to the contamination from substrates since electron spin resonance data clearly demonstrated that the substrate-free form of the enzyme accounted for more than 90% of the population (Griffin & Peterson, 1975; O'Keeffe et al., 1978b). We thus conclude that the distinction between the two Fe−CO species (α- and β-forms) in the substrate-free *b*-NOS must result from the intrinsic differences in the binding properties of CO and in the polar and/or steric effects exerted by the immediate environment of CO.

We propose that in substrate-free NO synthases, the bound CO with the β-conformation has a relatively open structure lacking either strong polar and/or steric constraints. The much lower ν_{Fe-CO} (486.7 cm^{-1}) and higher ν_{C-O} (1949.2 cm^{-1}) frequencies (i.e., closer to the right side in the ν_{Fe-CO}/ν_{C-O} correlation curve; Figure 8) in comparison to those from the α-form (∼501 and ∼1930 cm^{-1}, respectively; Table 1) support this argument (Ray et al., 1994; Wang et al., 1995a,b, 1996a). Such a flexible environment allows the bound CO to adopt multiple conformations. Indeed, the much broader line widths for ν_{Fe-CO} ($\Gamma_{1/2} = 26.5$ cm^{-1}) and ν_{C-O} ($\Gamma_{1/2} = 26.7$ cm^{-1}) for the β-form than those for the α-form of the enzyme ($\Gamma_{1/2} = 14-17$ and $14-23$ cm^{-1}, respectively) are in agreement with this proposal. Although the X-ray crystallographic structure for the CO adduct of cytochrome P-450$_{cam}$ in the absence of substrate is still not available, previous investigators have ascribed the CO conformation possessing a higher ν_{C-O} (1963 cm^{-1}) (β-form; see Table 1) as originating from a local structure with less electronic polarity and steric hindrance (O'Keeffe et al., 1978a; Jung et al., 1992). Indeed, the high yield (90%) of the geminate recombination for the CO adducts of substrate-free P-450$_{cam}$ with respect to the extremely low yield (2%) from its substrate-bound form, reported by Tian et al. (1995), is consistent with an "open" distal pocket for bound CO in β-form. In this case, the binding properties of bound CO is

not severely affected by its immediate environment and CO may bind to the heme iron in a linear orientation. A calculation by Jung et al. (1992) also suggests a nearly straight Fe−C−O linkage (angle between CO bond and heme normal, <5°) corresponding to the β-form of cytochrome P-450$_{cam}$. We propose that the β-form of *b*-NOS (in the substrate-free form) has an "open" distal pocket analogous to that present in the β-form of cytochrome P-450$_{cam}$ (Figure 9a), where the bound CO could also coordinate to the heme iron in a nearly linear orientation.

In the presence of a substrate (e.g., L-Arg or N^{ω}-OH-L-Arg) the binding conformation for bound CO in *b*-NOS differs appreciably from the substrate-free enzyme (β-form). Such a conversion leads to the complete α-form of the enzyme characterized by higher ν_{Fe-CO} (∼502 cm^{-1}) and lower ν_{C-O} frequencies (∼1929 cm^{-1}), indicating the strengthening in the electronic polarity or steric hindrance near the bound CO. The small line widths for the two marker lines in the substrate-bound form are consistent with the highly homogeneous local environment exerted by the existence of substrates. In cytochrome P-450$_{cam}$, the binding of substrate (camphor) results in shifts of both the ν_{Fe-CO} (from 464 to 481 cm^{-1}) and ν_{C-O} (from 1963 to 1940 cm^{-1}) modes with respect to those from the β-form in the substrate-free protein (O'Keeffe et al., 1978a; Uno et al., 1985; Jung et al., 1992).

Whether frequency shifts in the Fe−C−O moiety result from steric or polar effects was recently called into question. X-ray crystallographic data for the camphor-bound cytochrome P-450$_{cam}$−CO demonstrate that the bound CO is forced to bend and tilt away from the heme normal by 14° (Raag & Poulos, 1989). Meanwhile, camphor, H-bonded to Tyr-96, also moves away from heme iron by 0.8 Å in comparison to the CO-free form of the enzyme to accommodate the presence of the CO, maintaining a nonbonded distance to the heme-bound CO of 3.067 Å. On the basis of these X-ray and ν_{C-O} data from the camphor-bound form of cytochrome P-450$_{cam}$, Jung et al. (1992) calculated the average CO ligand orientation with respect to the heme normal, in conjunction with a linear correlation between the ν_{C-O} frequency and the angle of the CO bond to the heme normal derived from CO adducts of myoglobin (Ormos et al., 1988). They ascribed the substrate-induced transition in the CO-binding conformation (from β- to α-form) as arising from the steric hindrance caused by the presence of substrates, which forces bound CO to take a bent/tilted geometry (up to ∼29°) to accommodate the nearby substrates. However, the above correlation between the ν_{C-O} frequency and the angle of bound CO has been put into question, based on the newly reported crystal structure (Quillin et al., 1993) and infrared circular dichroism data (Ivanov et al., 1994; Lim et al., 1995) from CO adducts of myoglobins. They found that all the CO-binding conformations in myoglobin, albeit apparently distinct in their ν_{C-O} frequencies, have a virtually similar orientation with respect to the heme normal (all nearly linear). It has thus been concluded that the frequency shifts among the conformations of heme proteins are not primarily determined by the Fe−C−O distortion (steric effect) but are more sensitive to perturbations in the polarity of the distal pocket near the bound CO (Sakan et al., 1993; Ray et al., 1994; Li et al., 1994; Ivanov et al., 1994; Kushkuley & Stavrov, 1996). On the basis of the similarity of the conformational changes (an "open" form to a "closed" form) in the heme-bound CO between NO synthases, myoglobins, and cytochrome P-450$_{cam}$, we propose that the presence of L-Arg or N^{ω}-OH-L-Arg could exert a strong polar (and/or steric) effect on the bound CO thereby generating a closed distal pocket (model c in Figure 9).

The above argument is supported by the shifts of the ν_{Fe-CO} and ν_{C-O} upon the binding of camphor in cytochrome P-450$_{cam}$. They are quite substantial in view of the relatively small bending angle (14°) and the absence of H-bonding of CO with substrate as reported in the X-ray crystallographic results (Raag & Poulos, 1989). It should be noted that the oxygen atom of the bound CO is nestled into a groove formed by an unusual helical H-bonding between Thr-252 and Gly-248 (Raag & Poulos, 1989), which may account for the strong polar environment experienced by the CO molecule in substrate-bound cytochrome P-450$_{cam}$. In CPO, two CO-binding conformations are also evident by ν_{Fe-CO} and ν_{C-O} at 492 and 1942 cm^{-1} at pH ∼ 3 (O'Keeffe et al., 1978a; Bangcharoenpaurpong et al., 1986; Hu & Kincaid, 1993) but at 485 and 1957.5 cm^{-1} at pH ∼6 (Figure 6) (Hu & Kincaid, 1993). The frequency shifts were attributed to the presence of a strong interaction via H-bonding at pH 3 between the bound CO and distal residues which is disrupted by the pH increase (O'Keeffe et al., 1978a; Hu & Kincaid, 1993), despite the unavailability of the crystal structure for CPO(+2)−CO at either pH. For NOS, it is thus anticipated that a strong polar interaction such as a H-bonding may exist in its substrate-bound form. Indeed, our recent data indicate the formation of H-bonding to the heme-bound CO is associated with the binding of L-arginine to the distal pocket as well as a conversion from an "open" to a "closed" form (Wang et al., unpublished data).

Binding Sites in the Distal Pocket of b-NOS. We infer a highly polar, and crowded, distal environment for the CO molecule in the α-form of *b*-NOS in the presence of L-Arg or N^{ω}-OH-L-Arg. However, the most puzzling question is what causes nearly half of the CO population to bind to the heme iron in the α-conformation *in the absence of substrate*. It appears that the substrate binding site is occupied by some group in half of the population. This conclusion is supported by the CO binding rate constants determined by Matsuoka et al. (1994). They found that CO coordination to *b*-NOS is biphasic in the absence of substrate. The fast phase (rate constant: 1.9×10^5 M^{-1} s^{-1}), which accounted for only 40% of the total absorbance change, was attributed to a species lacking any interactions from the substrate (β-form). The slow phase has an association rate constant that is 8-fold smaller (2.3×10^4 M^{-1} s^{-1}) and is almost identical to that observed from the L-Arg bound enzyme (2.4×10^4 M^{-1} s^{-1}). Thus, in the substrate-free enzyme, the substrate binding site appears occupied in a fashion similar to that when the physiological substrate (L-Arg) is present. This occupancy result in the reduced CO on-rate and in the formation of the α-conformation.

As possible candidates for occupancy of the distal pocket in the absence of substrate we consider the following: (a) a water molecule/water cluster present in the substrate-free form of the enzyme; (b) the close proximity of BH_4 which may affect the binding properties of CO. In the substrate-free form of ferric cytochrome P-450$_{cam}$, an H-bonded water cluster coordinates to Fe^{3+} resulting in a 6C/LS heme iron (Dawson & Sono, 1987; Poulos et al., 1986). The addition of camphor to the enzyme blocks the water from coordinating

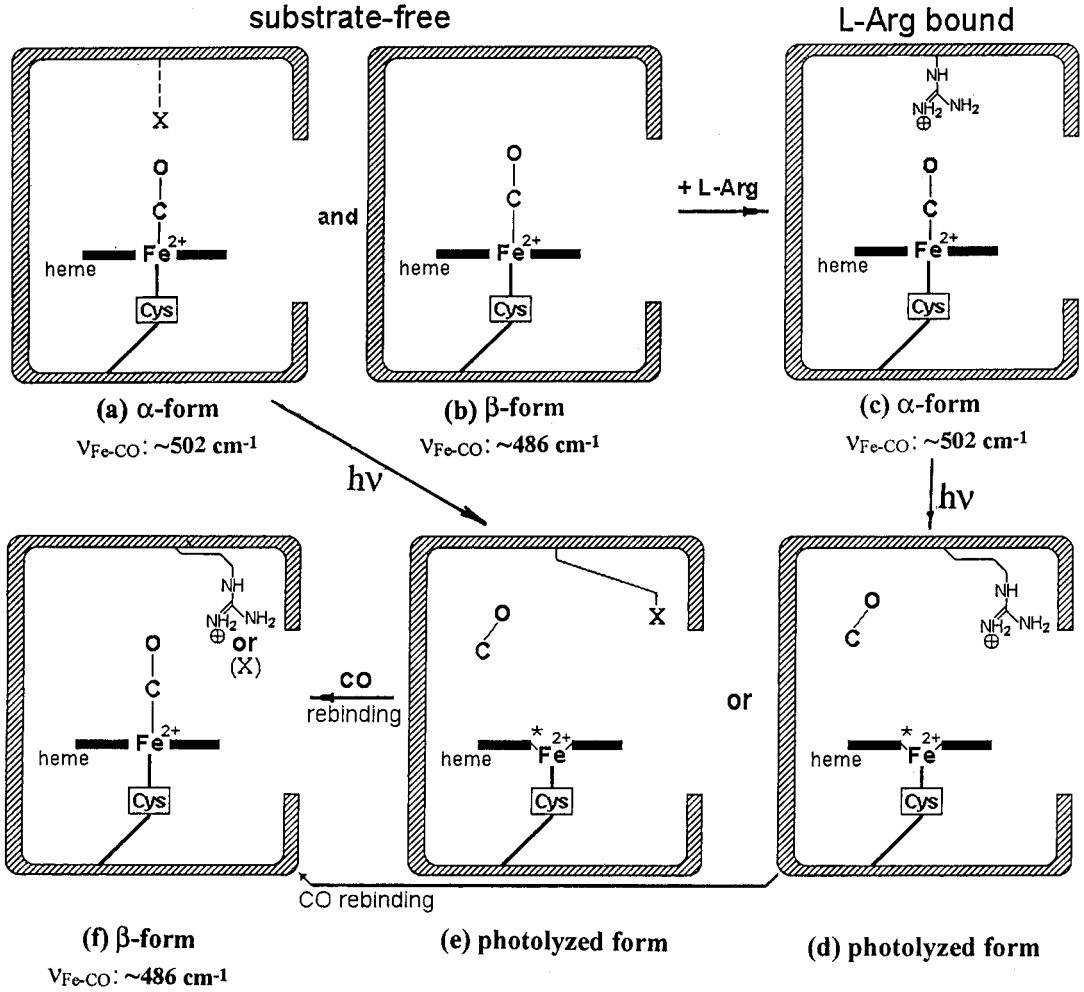

FIGURE 9: Scheme for the mechanism of CO photolysis and dependence of the Fe−C−O conformation on the presence of substrates or inhibitors in *b*-NOS. (a, b) The α- and *β*-conformations, respectively, of the Fe−C−O linkage in the substrate-free form of *b*-NOS. In the latter CO binds to the heme iron in a nearly linear orientation as a consequence of relatively open pocket, whereas in the former the pocket becomes more polar and/or crowded due to the presence of a hindering group such as BH_4, water or an amino acid residue (designated by X). (c) The addition of substrates such as L-arginine or N^{ω}-OH-L-arginine to substrate-free *b*-NOS−CO completely converts the "open" (*β*) Fe−C−O moiety to a homogeneous α-conformation. The current data cannot determine if L-arginine is competitive with the group X. (d, e) Two transient species produced by laser-induced photodissociation of CO from the α-conformation of substrate-bound or substrate-free forms of *b*-NOS−CO. In these cases, substrates (d) or the group X (e) may swing away or dissociate to allow the CO to diffuse from the site. (f) A photo-induced conversion from an α-conformation to a *β*-form of *b*-NOS−CO is produced since the photolyzed CO recombines to the heme iron at a rate faster than the return of the hindering group to its position in the distal pocket.

to the iron atom so that it becomes 5C/HS, but the pocket remains filled with loosely bonded or disordered water molecules (Poulos, 1986). It has been proposed (Jung et al., 1992) that when CO is bound to the substrate-free form of cytochrome-$P450_{cam}$, the water cluster still resides above it and thus affects its binding properties, although the crystal structure for it is not available at present. It is possible that a water molecule or H-bonded water cluster is also present in the distal pocket of *b*-NOS and is responsible for the nearly half the population adopting the α-conformation in its substrate-free form, although more direct evidence is required to firmly establish such effects.

An alternative origin for the α-structure in the substrate-free enzyme is the coordination of BH_4 in the heme pocket. Mayer and co-workers (Klatt et al., 1994, 1995) recently reported a 6-fold increase in the *b*-NOS affinity for BH_4 in the presence of L-arginine and also a 2-fold enhancement for the binding of N^{ω}-nitro-L-arginine in the presence of BH_4. These data also suggest an allosteric conformational change in *b*-NOS induced by both BH_4 and L-arginine, which may optimize both binding sites and thus lead to the enhanced affinities of both (Mayer & Werner, 1995). These data imply that BH_4 may bind to the distal pocket at a site as close to the heme as L-arginine does so that it can affect the binding properties of heme-bound ligand in a similar manner as L-arginine. Indeed, our recent Raman data show that, when the oxygen domain of *i*-NOS is prepared in the absence of BH_4, the α-conformation is markedly decreased and the *β*-form becomes predominant in its CO adducts (Wang et al., 1996b; Wang et al., unpublished data). Addition of BH_4 to the CO adduct of the BH_4-free oxygenase domain significantly restores the population in the α-conformation. Further experiments which may help to clarify this issue are underway.

It is very natural to argue that the same Raman frequencies for the "closed" structure in its L-arginine-bound and substrate-free forms may reflect a secondary effect on the heme-bound CO of NOSs, where L-Arg or BH_4 resides at a remote site and affects its CO-binding conformation through protein residues. In fact, the recent Raman data from human *i*-NOS (Wang et al., unpublished results) indicate that the magnitude of the frequency shifts (2−30 cm^{-1}) of CO-

associated lines depends on the structure of the inhibitors, thereby disfavoring a secondary effect.

Photodynamics and Interconversion of the Two CO-Conformers. We observed a laser-induced conversion from an α- to a *β*-conformation of the *b*-NOS-CO complex in both the L-Arg-bound (Figure 4) and the substrate-free forms (data not shown). Similar behavior was reported for CO-bound cytochrome P-450_{cam} (Wells et al., 1992). Champion and co-workers (Wells et al., 1992) ascribed this observation as a result of photolysis of the bound CO followed by an energy transfer from excited CO (CO*) to the protein-bound substrate thereby leading to its dissociation. In *b*-NOS the substrate (in the L-Arg-bound form) and some other group (designated by X) such as BH_4 or water (in the α-form of the substrate-free enzyme) are coordinated in the distal pocket and thus obstruct the dissociation and re-association of CO (models c and a in Figure 9, respectively). In order for CO to dissociate from the heme binding site and diffuse from the heme pocket, the substrate (e.g., in the L-Arg-bound form) or the hindering group (in the α-form of substrate free *b*-NOS) has to swing away or dissociate from its binding site. Such a process creates a transiently open pocket (models d and e) and thus results in the *β*-conformation upon the recombination of CO (model f) since the rebinding of CO is faster than the restoration of substrate or another group that occupies the substrate binding site.

Implications for b-NOS Reactivity. The current results offer new insights in catalysis by the heme of NO synthases. First, we extend prior studies (Wang et al., 1994; Matsuoka et al., 1994) by demonstrating the close proximity of the binding site of L-arginine analogues and inhibitors to the heme catalytic active site. While interactions between substrates and heme-bound ligand have been predicted by several catalytic models (Feldman et al., 1993; Marletta, 1993), the data we report here are consistent with those models, though more direct evidence is required to firmly establish the exact location of L-arginine and BH_4 in the distal pocket. Substrates, such as L-arginine and N^{ω}-OH-L-Arg, provide a highly homogeneous active site, leading to a complete high-spin (either penta- or hexacoordinate) heme structure available for coordination of the functional ligand, O_2 (McMillan & Masters, 1993; Pufahl & Marletta, 1993; Matsuoka et al., 1994). This facilitates the coordination which would be slower if a strong low-spin ligand had to be replaced. In addition, the binding site allows for the possibility that the end group of substrates or inhibitors may influence the electronic properties of the porphyrin ring and thus modify the redox potential of the heme iron as was observed in myoglobin when amino acid residues near the heme were mutated (Varadarajan et al., 1992; Wang et al., unpublished data). As the substrate binds quite close to the O_2 binding site, the polarity of substrates would be expected to significantly affect the stability of the activated oxygen which is necessary for the oxygenase activity.

A second important aspect of our results is the demonstration of two distinct types of heme environment: an "open" form (*β*-form) and a "closed" (α-form) form. The entire enzyme population adopts the latter form when substrate is present, but 50% of the enzyme adopts the α-form in the absence of substrate. The functional significance of a structure in which the substrate binding site appears occupied even in the absence of substrate cannot be assessed at present. However, it is well-known that enzymes exhibit dynamic structures (Koshland, 1976) so the two structures in the absence of substrate could represent a dynamic interconversion between an "open" and a "closed" structure (Tian et al., 1993). Dynamic processes could have kinetic consequences on the catalytic function as suggested by the differing on-rates for CO association (Matsuoka et al., 1994). Recently, Champion and co-workers (Tian et al., 1996) reported the interconversion time (10^{-6}−10^{-4} s) between the "open" and "closed" structures in myoglobin, which is significantly affected by the viscosity and temperature of the medium. The exchange rate is not known for NOS at present. If the interconversion between the two conformations is fast enough and compatible with the time range for the catalytic events of NOS, a switch between the two conformations may occur in the catalysis and thereby regulate the recruiting of the substrates and ligand as well as the departure of the products. If the interchange between the states is slow, however, the two distinct heme populations may not play identical roles in the complex catalysis.

ACKNOWLEDGMENT

We thank Dr. P. Feldman from Glaxo for the kind donation of L-thiocitrulline. We also thank Drs. G. Paris and B. Fan for the exciting discussions. The Raman measurements were made while J.W. and D.L.R. were at AT&T Bell Laboratories.

REFERENCES

Abu-Soud, H. M., & Stuehr, D. J. (1993) *Proc. Natl. Acad. Sci. U.S.A. 90*, 10769−10772.

Abu-Soud, H. M., Feldman, P. L., Clark, P., & Stuehr, D. J. (1994) *J. Biol. Chem. 269*, 32318−32326.

Baek, K. J., Thiel, B. A., Lucas, S., & Stuehr, D. J. (1993) *J. Biol. Chem. 268*, 21120−21129.

Bangcharoenpaurpong, O. (1987) Ph.D. Dissertation, Northeastern University, Boston, MA.

Bangcharoenpaurpong, O., Champion, P. M., Hall, K. S., & Hager, L. P. (1986) *Biochemistry 25*, 2374−2378.

Benko, B., & Yu, N.-T. (1983) *Proc. Natl. Acad. Sci. U.S.A. 80*, 7042−7046.

Bredt, D. S., Hwang, P. M., Glatt, C. E., Lowenstein, C., Reed, R. R., & Snyder, S. H. (1991) *Nature 351*, 714−718.

Champion, P. M. (1988) in *Biological Applications of Raman Spectroscopy* (Spiro, T. G., Ed.) Vol. 3, pp 249−292, John Wiley & Sons, New York.

Champion, P. M., Stallard, B. R., Wagner, G. C., & Gunsalus, I. C. (1982) *J. Am. Chem. Soc. 104*, 5469−5472.

Chen, P.-F., Tsai, A.-L., & Wu, K. K. (1994) *J. Biol. Chem. 269*, 25062−25066.

Culotta, E., & Koshland, D. S. (1992) *Science 258*, 1862−1865.

Dasgupta, S., Rousseau, D. L., Anni, H., & Yonetani, T. (1989) *J. Biol. Chem. 264*, 654−662.

Dawson, J. H., & Sono, M. (1987) *Chem. Rev. 87*, 1255−1276.

Feldman, P. L., Griffith, O. W., & Stuehr, D. J. (1993) *Chem. Eng. News 71* (51), 26−38.

Feelisch, M., & Stamler, J., Eds. (1996) *Methods in Nitric Oxide Research*, John Wiley & Sons, Chichester, U.K.

Förstermann, U., Nakane, M., Tracey, W. R., & Pollock, J. S. (1993) *Eur. Heart J. 14* (Suppl. 1), 10−15.

Frey, C., Narayanan, K., McMillan, K., Spack, L., Gross, S. S., Masters, B. S. S., & Griffith, O. W. (1994) *J. Biol. Chem. 269*, 26083−26091.

Furchgott, R. F. (1988) in *Vasodilation: Vascular Smooth Muscle, Peptides, Autonomic Nerves, and Endothelium* (Vanhoutte, P. M., Ed.) pp 401−414, Raven, New York.

Ghosh, D. K., & Stuehr, D. J. (1995) *Biochemistry 34*, 801−807.

Griffin, B. W., & Peterson, J. A. (1975) *J. Biol. Chem. 250*, 6445−6451.

Griffith, O. W., & Stuehr, D. J. (1995) *Annu. Rev. Physiol. 57*, 707−736.

Hevel, J. M., & Marletta, M. A. (1992) *Biochemistry 31*, 7160−7165.

Hibbs, J. B., Jr., Vavrin, Z., & Taintor, R. R. (1987) *J. Immunol. 138*, 550−565.

Hirota, S., Ogura, T., Shinawa-Itoh, K., Yoshikawa, S., Nagai, M., & Kitagawa, T. (1994) *J. Phys. Chem. 98*, 6652−6660.

Hu, S., & Kincaid, J. R. (1991) *J. Am. Chem. Soc. 113*, 2843−2850.

Hu, S., & Kincaid, J. R. (1993) *J. Biol. Chem. 268*, 6189−6193.

Ignarro, L. J., & Murad, F., Eds. (1995) *Adv. Pharmacol., Vol. 34, Nitric Oxide: Biochemistry, Molecular Biology*, and *Therapeutic Implications*, Academic Press, New York.

Ignarro, L. J., Byrns, R. E., & Woods, K. S. (1988) in *Vasodilation: Vascular Smooth Muscle, Peptides, Autonomic Nerves, and Endothelium* (Vanhoutte, P. M., Ed.) pp 427−435, Raven, New York.

Ivanov, D., Sage, J. T., Meim, M., Powell, J. R., Asher, S. A., & Champion, P. M. (1994) *J. Am. Chem. Soc. 116*, 4139−4140.

Jung, C., Hui Bon Hoa, G., Schroder, K.-L., Simon, M., & Doucet, J. P. (1992) *Biochemistry 31*, 12855−12862.

Klatt, P., Schmid, M., Leopold, E., Schmidt, K., Werner, E. R., & Mayer, B. (1994) *J. Biol. Chem. 269*, 13861−13866.

Klatt, P., Schmidt, K., Lehner, D., Glatter, O., Bächinger, H. P., & Mayer, B. (1995) *EMBO J. 14*, 3687−3695.

Klatt, P., Pferffer, S., List, B. M., Lehner, D., Glatter, O., Bachinger, H. P., Werner, E. R., Schmidt, K., & Mayer, B. (1996) *J. Biol. Chem. 271*, 7336−7342.

Koshland, D. E., Jr. (1976) *FEBS Lett. 62*, E47−E52.

Kushkuley, B., & Stavrov, S. S. (1996) *Biophys. J. 70*, 1214−1229.

Lancaster, J. R., Jr. (1992) *Am. Sci. 80*, 248−259.

Li, T., Quillin, M. L., Phillips, G. N., Jr., Olson, J. S. (1994) *Biochemistry 33*, 1433−1446.

Lim, M., Jackson, T. A., & Anfinrud, P. A. (1995) *Science 269*, 962−966.

Marletta, M. A. (1993) *J. Biol. Chem. 268*, 12231−12234.

Marletta, M. A., Yoon, P. S., Iyengar, R., Leaf, C. D., & Wishnok, J. D. (1988) *Biochemistry 27*, 8706−8711.

Matsuoka, A., Stuehr, D. J., Olson, J. S., Clark, P., & Ikeda-Saito, M. (1994) *J. Biol. Chem. 269*, 20335−20339.

Mayer, B., & Werner, E. R. (1995) in *Adv. Pharmacol., Vol. 34, Nitric Oxide: Biochemistry, Molecular Biology, and Therapeutic Implications* (Ignarro, L. J., & Murad, F., Eds.) pp 251−261, Academic Press, New York.

McMillan, K., & Masters, B. S. S. (1993) *Biochemistry 32*, 9875−9880.

McMillan, K., & Masters, B. S. S. (1995) *Biochemistry 34*, 3686−3693.

McMillan, K., Bredt, D. S., Hirsch, D. J., Snyder, S. H., Clark, J. E., & Masters, B. S. S. (1992) *Proc. Nat. Acad. Sci. U.S.A. 89*, 11141−11145.

Moncada, S., Palmer, R. M. J., & Higgs, E. A. (1988) *Hypertension 12*, 365−372.

O'Keeffe, D. H., Ebel, R. E., Peterson, J. A., Maxwell, J. C., & Caughey, W. S. (1978a) *Biochemistry 17*, 5845−5852.

O'Keeffe, D. H., Ebel, R. E., & Peterson, J. A. (1978b) *Methods Enzymol. 52*, 151−157.

Ormos, P., Ansari, A., Braunstein, D., Cowen, B. R., Frauenfelder, H., Hong, M. K., Iben, I. E. T., Sauke, T. B., Steinbach, P. J., & Yong, R. D. (1988) *Biophys. J. 57*, 191−199.

Poulos, T. L. (1986) in *Cytochrome P-450, Structure, Mechanism and Biochemistry* (Ortiz de Montellano, P. R., Ed.) pp 505−539, Plenum Press, New York.

Poulos, T. L. (1996) *J. Biol. Inorg. Chem. 1*, 356−359.

Poulos, T. L., Finzel, B. C., Gunsalus, I. C., Wagner, G. C., & Kraut, J. (1985) *J. Biol. Chem. 260*, 16122−16130.

Poulos, T. L., Finzel, B. C., & Howard, A. J. (1986) *Biochemistry 25*, 5314−5322.

Proniewicz, L. M., & Kincaid, J. R. (1990) *J. Am. Chem. Soc. 112*, 675−681.

Pufahl, R. A., & Marletta, M. A. (1993) *Biochem. Biophys. Res. Commun. 193*, 963−970.

Quillin, M. L., Arduini, R. M., Olson, J. S., & Phillips, G. N., Jr. (1993) *J. Mol. Biol. 234*, 140−155.

Raag, R., & Poulos, T. L. (1989) *Biochemistry 28*, 7586−7592.

Ray, G. B., Li, X.-Y., Alers, J. A., Sessler, J. L., & Spiro, T. G. (1994) *J. Am. Chem. Soc. 116*, 162−176.

Richards, M. K., & Marletta, M. A. (1994) *Biochemistry 33*, 14723−14732.

Rodriguez-Crespo, I., Gerber, N. C., & Ortiz de Montellano, P. R. (1996) *J. Biol. Chem. 271*, 11462−11467.

Rousseau, D. L., Ching, Y.-C., & Wang, J. (1993) *J. Bioenerg. Biomembr. 25*, 165−176.

Sakan, Y., Ogura, T., Kitagawa, T., Frauenfelder, H., Mattera, R., & Ikeda-Saito, M. (1993) *Biochemistry 32*, 5815−5824.

Salerno, J. C., Frey, C., McMillan, K., Williams, R. F., Masters, B. S. S., & Griffith, O. W. (1995) *J. Biol. Chem. 270*, 27423−27428.

Sampath, V., Rousseau, D. L., & Caughey, W. S. (1996) in *Methods in Nitric Oxide Research* (Feelisch, M., & Stamler, J., Eds.) pp 413−426, John Wiley & Sons, Chichester, U.K.

Sessa, W. C. (1994) *J. Vasc. Res. 31*, 131−143.

Snyder, S. H., & Bredt, D. S. (1992) *Sci. Am. 266*, 68−77.

Spiro, T. G., Smulevich, G., & Su, C. (1990) *Biochemistry 29*, 4497−4508.

Stamler, J. S., Singel, D. S., & Loscalzo, J. (1992) *Science 258*, 1898−1902.

Stuehr, D. J., & Nathan, C. F. (1989) *J. Exp. Med. 169*, 1543−1555.

Stuehr, D. J., & Ikeda-Saito, M. (1992) *J. Biol. Chem. 267*, 20547−20550.

Stuehr, D. J., Gross, S. S., Sakuma, I., Levi, R., & Nathan, C. F. (1989) *J. Exp. Med. 169*, 1011−1020.

Tian, W. D., Sage, T., & Champion, P. M. (1993) *J. Mol. Biol. 233*, 155−166.

Tian, W. D., Wells, A. V., Champion, P. M., Primo, C. D., Gerber, N., & Sligar, S. G. (1995) *J. Biol. Chem. 270*, 8673−8679.

Tian, W. D., Sage, T., Champion, P. M., Chien, E., & Sligar, S. G. (1996) *Biochemistry 35*, 3487−3502.

Tzeng, E., Billiar, T. R., Robbins, P. D., Loftus, M., & Stuehr, D. J. (1995) *Proc. Natl. Acad. Sci. U.S.A. 92*, 11771−11775.

Uno, T., Nihsimura, Y., Makino, R., Iizuka, T., Ishimura, Y., & Tsuboi, M. (1985) *J. Biol. Chem. 260*, 2023−2026.

Varadarajan, R., Zewert, T. E., Gray, H. B., & Boxer, S. G. (1989) *Science 243*, 69−72.

Wang, J., Boldt, N. J., & Ondrias, M. R. (1992) *Biochemistry 31*, 867−878.

Wang, J., Stuehr, D. J., Ikeda-Saito, M., & Rousseau, D. L. (1993) *J. Biol. Chem. 268*, 22255−22258.

Wang, J., Rousseau, D. L., Abu-Soud, H. M., & Stuehr, D. J. (1994) *Proc. Natl. Acad. Sci. U.S.A. 91*, 10512−10516.

Wang, J., Stuehr, D. J., & Rousseau, D. L. (1995a) *Biochemistry 34*, 7080−7087.

Wang, J., Takahashi, S., Rousseau, D. L., Hosler, J. P., Ferguson-Miller, S., Mitchell, D. M., Gennis, R. B. (1995b) *Biochemistry 34*, 9819−9825.

Wang, J., Takahashi, S., & Rousseau, D. L. (1995c) *Proc. Natl. Acad. Sci. U.S.A. 92*, 9402−9406.

Wang, J., Caughey, W. S., & Rousseau, D. L. (1996a) in *Methods in Nitric Oxide Research* (Feelisch, M., & Stamler, J., Eds.) pp 427−454, John Wiley & Sons, Chichester, U.K.

Wang, J., Wu, C., Ghosh, D. K., Zhang, J., Stuehr, D. J., & Rousseau, D. L. (1996b) in *Fifteenth International Conference on Raman Spectroscopy* (Asher, S. A., & Stein, P., Eds.) pp 440−441, John Wiley & Sons, Chichester, U.K.

Wells, A. V., Li, P., Champion, P. M., Martinis, S. A., & Sligar, S. G. (1992) *Biochemistry 31*, 4384−4393.

Yu, N.-T., & Kerr, E. A. (1988) in *Biological Applications of Raman Spectroscopy* (Spiro, T. G., Ed.) Vol. 3, pp 39−95, John Wiley & Sons, New York.

BI962309U